WARSAW UNIVERSITY OF TECHNOLOGY Index 351733
FACULTY OF CIVIL ENGINEERING
COMMITTEE FOR CIVIL AND WATER ENGINEERING
POLISH ACADEMY OF SCIENCES ISSN 1230-2945

DOI: 10.24425/ace.2025.154135

ARCHIVES OF CIVIL ENGINEERING

Vol. LXXI ISSUE 2 2025

pp. 521–536

Research paper

Comparative evaluation of concrete constitutive models in blast loaded shaped structural units

Sreekumar Punnappilly[1], Baskar Kaliyamoorthy[2]

Abstract: The displacement response of a cylindrical and an apsidal shaped structural unit under blast loading is compared in this study using the finite element code LS-DYNA utilizing two different concrete constitutive models, namely the Riedel–Hiermaier–Thoma (RHT) model and the Continuous Surface Cap Model (CSCM). The blast load generated by an emulsion explosive corresponding to six scaled distances is used for the study. The validation of the displacement response is carried out by utilizing the Newmark numerical integration procedure using the linear acceleration method. The unique apsidal shape in its displacement response performs better across all the simulations indicating superior blast resistance. CSCM model returns conservative values of displacements in the study. The study finds that the RHT model requires higher stress levels for consideration of dynamic strengths and hence returns lower displacement values for the instances considered in this simulation. This study recommends the use of an apsidal unit and the use of RHT constitutive model in the simulations.

Keywords: acceptor structure, apsidal unit, blast load, CSCM model, cylindrical unit, RHT model

[1]MSc., Research Scholar, Department of Civil Engineering, National Institute of Technology, Tiruchirappalli, Tamil Nadu 620015, India, e-mail: sreekumaracademic@gmail.com, ORCID: 0000-0001-6778-2252

[2]Professor, Department of Civil Engineering, National Institute of Technology, Tiruchirappalli, Tamil Nadu 620015, India, e-mail: kbaskar@nitt.edu, ORCID: 0000-0003-2967-9267

1. Introduction

There is an ever present need to study the effect of blast loading on structures. This is a direct result of the incidents of deliberate and accidental explosions affecting civil engineering structures. The structures are affected in adverse ways by the blast loads. Some of the explosions are intended to result in catastrophic structural response. Even without a total collapse of the acceptor structure, the deleterious structural responses can be quite damaging to the structural health.

Research work, both past and present, points to the extensive quantum of work done in the field of blast loading on structures. Both experimental methods and numerical analysis have been employed in this regard. Research work on a wide variety of construction materials and composites is available. Deflection of the structural components is an important aspect of the structural response when subjected to blast loads. Further, the geometry of the acceptor structural unit also plays a key role in the structural response.

There are only limited studies on the influence of structural shapes on the blast loads and their effects. However, there have been numerous studies on the effect of blast and impact loads on concrete structures of regular shapes. The nonlinear dynamic response of arching masonry walls under blast loads has been studied by Edri *et al.* [1]. Experimental results from the study provide a better understanding of the blast response and serve to validate the numerical models. Experimental and numerical studies on tubular concrete structures under blast loading have been conducted by Kristoffersen *et al.* [2]. The research concluded that explosive charges with confinement caused more damage involving longitudinal cracking and fragmentation. The work by Fallon and McShane [3] numerically investigates the fluid-structure interaction effect experienced by an elastomer-coated concrete slab subjected to blast loads. It was found that the elastomer coating improves blast resistance. The results also indicate that the use of a purely Lagrangian approach, in which a pressure–time history is directly applied to the acceptor structure, captures the structural response of the specimens. The behavior of a concrete slab perforated by a deformable bullet is the subject of numerical and experimental investigation in the research by Baranowski *et al*. [4]. The research utilizes experimental and numerical methods for the determination and correlation of the constitutive model parameters and provides insights into the failure behavior of a concrete slab. The effect of blast loads on concrete structures is studied in the work by Ibrahim and Almustafa [5], considering composite columns and structures retrofitted with braces. They have noted that the structures with composite columns and steel braced structures experienced less blast damage. The effect of blast loads on concrete structures and their foundations in a real-life scenario is studied in the research work by Ismail *et al*. [6]. The field data from the actual catastrophic events is compared with the numerical models and the study concludes detailing the high level of damage caused and the unsuitability of the foundations for possible future reuse.

Constitutive models represent the materials in the finite element analysis field. For structural concrete the commonly used constitutive models for dynamic loading includes among others, Riedel–Hiermaier–Thoma (RHT) model, Continuous Surface Cap Model (CSCM)and the

Karagozian and Case concrete model. The work by Kucewicz *et al*. [7] provides a detailed comparison of the commonly used material models including the three models mentioned previously and the experimental methods used for the determination of the model parameters and their evaluation. Extensive work is documented in relation to dynamic fragmentation of dolomite rock and the comparative evaluation of three material models is presented. The CSCM and RHT models have been used in the study by Reifarth *et al*. [8] on the performance of blast loaded externally reinforced concrete slabs. The research work indicates that CSCM model provides for accurate and easy modelling of reinforced concrete subjected to blast tests. The study utilized the Load Blast Enhanced keyword in LS-DYNA for the numerical simulation.

Blast loading involves the interaction of the structure with the components of the blast wave. Proper coupling of these two components is essential in a blast analysis. The research paper by Teich and Gebbeken [9] investigates the influence of fluid-structure interaction (FSI) on the structural response of systems subjected to blast loads. The paper indicates that the load acting on the system depends on the deformation of the system and vice versa. In a different scenario, the work by Baranowski *et al*. [10] examines the various facets of gas -body coupling by subjecting a pneumatic tire to a blast wave. The paper studies the dynamic response of a tire subjected to blast loads with different cord configurations. The utilization of a FSI interface is also highlighted in the paper by Mazurkiewicz *et al.* [11] wherein a method of sandwich protective panel optimization based on computational mechanics is presented. The study verified the obtained parameters using full finite element model of protective panel and pillar with FSI interface.

Numerical simulations are widely used in blast studies due to the inherent issues involved in experimental research. LS-DYNA is a widely used finite element program adopted for this work. LS-DYNA is a proven dynamic program that has been used to study the dynamic response of structural concrete units subjected to blast loads [12–16]. Further economic factors limited the ability of authors to carry out experimental validation of the finite element results. Hence analytical methods were resorted to for validation purposes.

Some of the early works on exploring the relationship between structural shapes and blast effects are found in [17–19]. The authors were so far unable to locate recent works on this specific aspect of blast loading effects on shaped structural units. This denotes a research gap, and this paper represents a preliminary attempt to study the effects of blast loads on shaped structural units.

The selection of the two distinct shapes in this study is to address the need for study of specific structural shapes in blast loading. Out of this the apsidal shape suggested is unique and was found unavailable in the literature survey by the authors. The displacement response is a key factor in the design of blast resistant structures. Two constitutive models have been adapted here namely the RHT model and the CSCM model. Thus, the research has attempted to evaluate the specific structural shapes under different blast loads and with varying constitutive models which has not been attempted so far as indicated in the literature survey by the authors. Thus, it can be considered that this study marks a unique and novel research trail which can easily be followed by subsequent researchers in the field.

2. Constitutive material models

The finite element codes use material models to precisely simulate the dynamic material properties of concrete. For this work, the two constitutive models considered are the Riedel–Hiermaier–Thoma (RHT) model and the Continuous Surface Cap Model (CSCM). Both these models support nonlinear elasticity, and the relevant details are elaborated in the following sections.

2.1. Riedel–Hiermaier–Thoma model

The RHT model is a material model that gives an appropriate dynamic strength description of concrete at impact relevant strain rates and pressures. The model employs three shear strength surfaces, the inelastic yield surface, the failure surface and the residual surface, all dependent on pressure [20]. This model is the result of the coupling of an equation of state indicating the porous compaction of concrete and a strength model. The volumetric compaction model adopted here is shown in Fig. 1. p_{crush} indicates the pore crush pressure and p_{comp}, the compaction pressure. ε_{vol} is the volumetric strain. The model exhibits elastic behavior below the pore crush pressure. α is an internal variable representing the material's porosity and is the ratio of the densities of the matrix material and porous concrete. When the pressure reaches $p_{comp,}$ the material is assumed to be fully compacted, implying $\alpha = 1$, and will be governed by a conventional equation of state [20].

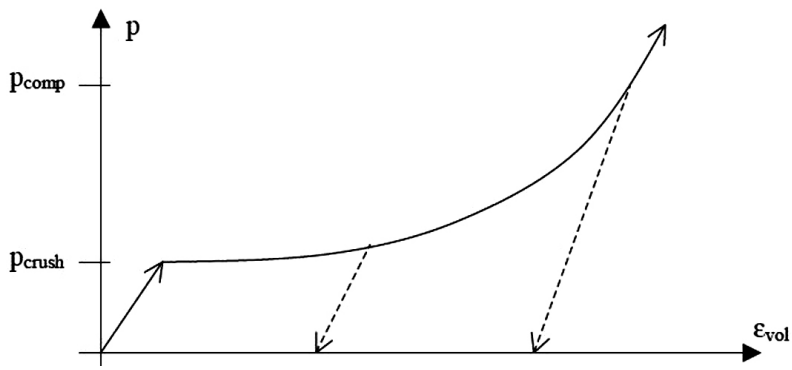

Fig. 1. Schematic description of the p-α equation of state [20]

The RHT strength model comprises three stress limit surfaces, namely the inelastic yield surface, the failure surface and the residual surface, as shown in Fig. 2. Elastic behavior exists until the yield surface is reached. Thereafter, plastic strains develop, which serve as one of the inputs for obtaining the effective yield surface, which is arrived at by interpolating between the initial yield surface and the failure surface.

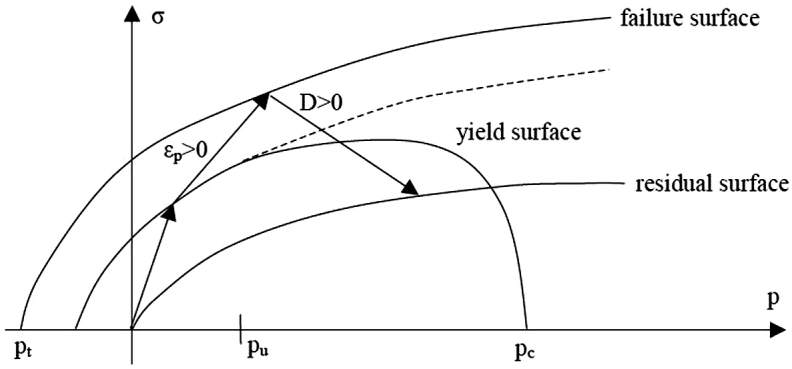

Fig. 2. Stress limit surfaces and loading scenario in the RHT strength model [20]

2.2. Continuous Surface Cap Model

CSC model is a cap model with a continuous intersection between the failure surface and the hardening cap [21]. The surface combines the failure surface with the hardening compaction surface in a smooth manner.

The yield surface is defined by three stress invariants: J_1 – the first invariant of the stress tensor, $J_2^{'}$ – the second invariant of the deviatoric stress tensor, and $J_3^{'}$ – the third invariant of the deviatoric stress tensor. These invariants are defined by the deviatoric stress tensor, S_{ij} and pressure P as described in the Eq. (2.1), (2.2) and (2.3).

$$J_1 = 3P \tag{2.1}$$

$$J_2^{'} = \frac{1}{2} S_{ij} S_{ij} \tag{2.2}$$

$$J_3^{'} = \frac{1}{3} S_{ij} S_{jk} S_{ki} \tag{2.3}$$

In this constitutive model, the rate effects are modelled with viscoplasticity.

3. Acceptor structure

The acceptor structure models are of two distinct shapes, namely cylindrical and apsidal. A small-scale model of overall height 800 mm is considered. The structure is of reinforced concrete with a compressive strength of 35 MPa. The concrete is reinforced with 8 mm bars double layered at 250 mm centers in both directions. The structural units have a uniform thickness of 150 mm. A constraint fixity is provided for a depth of 200 mm as the boundary condition.

The structural units are shown in Fig. 3 and Fig. 4, where all the dimensions are in units of mm.

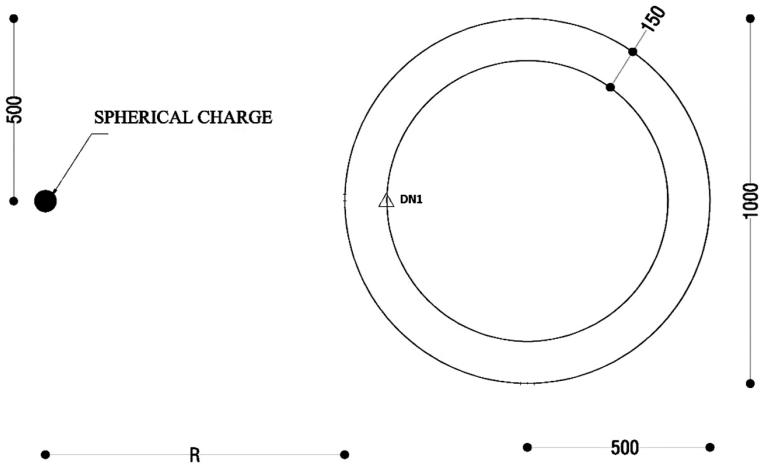

Fig. 3. Cylindrical unit

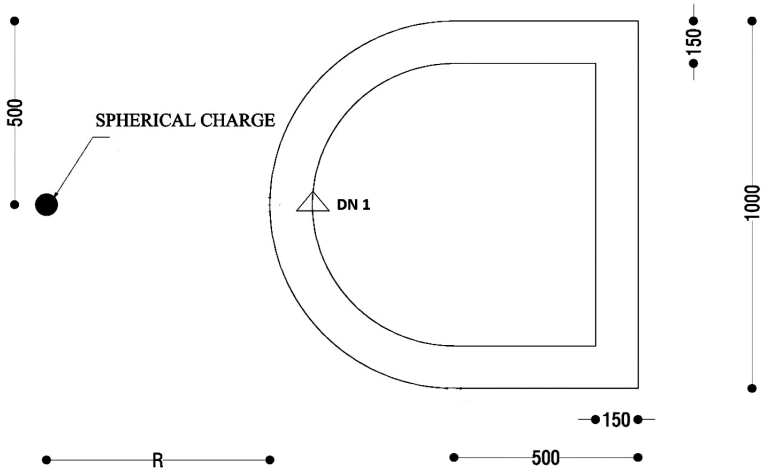

Fig. 4. Apsidal unit

The finite element simulation described in the subsequent sections results in the evaluation of the nodal displacement at DN1, located on the top inner face of the concrete units. The location of DN1 is indicated on the concrete units in Fig. 3 and Fig. 4.

4. Finite element simulation

The finite element simulations are carried out using the nonlinear general purpose finite element code LS-DYNA. Lagrangian approach is adopted in the study employing the keyword LOAD_BLAST_ENHANCED. This keyword utilizes tables of experimental data for conven-

tional explosions converted into approximating polynomials using classical scaling laws [22]. The finite element simulation utilizes hexahedral constant stress solid elements for modelling the concrete units. The rebars are modelled using Hughes – Liu beam elements with cross-section integration. An element size of 12.5 mm is adopted for all the simulations in this study.

4.1. Blast load

The blast load is generated employing an emulsion explosive named Superpower 90 [23], which is used in commercial blasting operations. As per the datasheet, the explosive has an effective energy (Q_x) of 166% of ANFO. Since ANFO has an effective energy of 2300 kJ/kg, Q_x can be evaluated as equal to 3818 kJ/kg. The TNT equivalence is the ratio of the effective energy of the explosive to that of TNT (Q_{TNT}). Since TNT has an effective energy of 4520 kJ/kg, the TNT equivalence of the explosive is deduced to be equal to 0.845. This study considers two distinct charge weights of 1.0 and 1.56 kg of the spherically shaped emulsion explosive. The standoff distances considered are 1.25, 1.5 and 1.75 m. The TNT equivalent weights of the explosive charges are 0.845 and 1.318 kg, respectively. The corresponding scaled distances computed using the cube root scaling law are 1.140, 1.322, 1.368, 1.587, 1.596 and 1.851 m/kg$^{1/3}$ in the ascending order of their magnitudes. The layout showing the positioning of the explosive charges for the structural units are shown in 3 and Fig. 4. The centre of the explosive charge for all the simulations is kept at a depth of 300 mm from the top face of the structural units.

4.2. Materials

4.2.1. Material model for steel

The material model considered for steel rebars is the MAT_PLASTIC_KINEMATIC model. It is suitable for modelling isotropic and kinematic hardening plasticity with the option of including rate effects. Strain rate is accounted for using the Cowper and Symonds model which scales the yield stress. The material properties input during the analysis for a commonly used rebar material are given in Table 1.

Table 1. Properties of steel

Mass density (ρ)	**Young's Modulus E**	**Poisson's ratio**	**Yield stress**
7.85×10^{-6} kg/mm^3	207 GPa	0.3	0.5 GPa

4.2.2. Material model for concrete

For the concrete structural unit, the material models considered are the RHT model and the CSCM model, described in detail in Section 2. The parameters associated with the constitutive models define the material and its behaviour. For the RHT model, the parameter values attributed to a concrete material of 35 MPa compressive strength from [20] are adopted.

For the CSCM model, the automatic parameter generation option available in LS-DYNA has been utilised which provides the parameters based on the input of unconfined compression strength of concrete and its density. The properties input for the structural unit in the simulations are:

1. Density – RO – 2.314×10^{-6} kg/mm^3,
2. Unconfined compression strength $f_c^{'}$ – FPC – 0.035 GPa.

5. Results and discussions

The results from the finite element simulations for the two distinct structural shapes subjected to identical blast loads are discussed here. The displacement of the node DN1 for each of the twenty four simulations is compared for the variations due to the shape of the structural units as well as due to the choice of the constitutive model for the concrete.

5.1. Validation of the FE model

The validation of the results is carried out in a theoretical way in two steps as detailed in this section. In the first part, the incident pressure, which is the effect of the explosion on the structure is validated. In the second part, the displacement response of an analogous model is obtained employing the Newmark numerical integration procedure and comparing with the results from the finite element model. This serves to validate the constitutive parameters of the model.

5.1.1. Validation of the incident pressures

The theoretical values of the incident pressure are calculated using the Henrych formula [24] and utilized to validate the model. The Henrych formula relates the scaled distance and the incident blast pressure, and this formula for a scaled distance between 1 and 10 m/kg$^{1/3}$ is given by

$$\Delta p_{\varphi} = \frac{0.662}{\bar{R}} + \frac{4.05}{\bar{R}^2} + \frac{3.288}{\bar{R}^3} \text{kgf/cm}^2 \tag{5.1}$$

where Δp_{φ} is the maximum overpressure at the shock wave front, and $\bar{R}$ denotes the scaled distance in m/kg$^{1/3}$.

A comparison of the theoretical values and the results from the finite element model (RHT) for the cylindrical unit is provided in Table 2. The comparison is carried out for the incident pressure on the frontal face of the cylindrical unit in line with the explosive charge.

It can be inferred from the above table that the corresponding values are in agreement with the mean variation of only 8%. Hence, the FE model considered here is found to be validated and utilized for further analysis of the displacement parameter, which is directly related to the incident pressure resulting from the explosive blast.

5.1.2. Validation of the displacement response

The validation of the displacement response is carried out by utilising the Newmark numerical integration procedure using the linear acceleration method [25]. An analogous

Table 2. Comparison of validation results for incident pressures

Scaled distance ($m/kg^{1/3}$)	Incident pressure (kPa) from FE model (RHT)	Incident pressure (kPa) using the Henrych formula
1.140	684.53	580.20
1.322	413.09	415.92
1.368	396.87	385.63
1.587	325.52	279.28
1.596	289.53	275.91
1.851	228.96	201.84

structural model is chosen, which is a rectangular concrete wall 1000 mm wide and 800 mm high and fixed for a depth of 200 mm bottom and considered as a cantilever wall spanning in the vertical direction. The reinforcement consists of 8 mm bars double layered at 250 mm centres in both the directions. All the material used in this model matches exactly with the simulation models studied in this work. The structural unit is subjected to the same blast load as detailed in Section 4.1.

The structure is approximated as a single degree of freedom (SDOF) entity and a triangular loading approximates the blast load. The blast parameters pertaining to the various scaled distances are obtained from UFC 3-340-02 [26]. The bending resistance for the structural unit is worked out considering the strength and dynamic increase factors for both concrete and steel. The load -mass transformation factor K_{LM} is used to calculate the equivalent mass, stiffness and loading of the equivalent SDOF system [25]. This ensures that both the elastic and plastic phases of the deformation are accounted for. The values are run through the numerical integration procedure and the displacements are compared to those obtained from the LS-DYNA simulation in Table 3.

Table 3. Comparison of validation results for displacement response

Scaled distance ($m/kg^{1/3}$)	Displacement (mm) from FE model (RHT)	Displacement (mm) from the numerical integration
1.140	42.03	54.23
1.322	18.54	16.39
1.368	21.49	16.86
1.587	8.53	6.41
1.596	10.73	8.1
1.851	3.0	3.27

The comparison shows that the displacement values differ by an average of 7.4%, Considering that simplifying structural assumptions are used, the results can be considered as in moderate agreement.

Both the validations support the premise of proceeding with the further finite element simulations in this research work.

5.2. Structural unit wise comparison

The displacement at the designated node is compared for the two distinct structural units, namely cylindrical and apsidal, in the accompanying Table 4. The displacement values are higher for the cylindrical unit for all the cases of blast loading. The cylindrical unit experiences higher displacements under blast loading. The simulations utilizing the RHT constitutive model of concrete indicate an average increase of 21.40% in the displacement values for the cylindrical unit relative to that of the apsidal unit. The corresponding average increase for the simulations involving the CSCM model is 31.64%. The cylindrical unit undergoes larger displacements under blast loading scenarios considered here.

Table 4. Peak displacement comparison – Structural unit wise

Concrete constitutive model	**Charge weight (kg)**	**Standoff distance *R* (m)**	**Peak displacement at DN1 (mm)**	
			cylindrical Unit	**apsidal Unit**
RHT	1.0	1.25	0.64	0.52
		1.5	0.38	0.35
		1.75	0.27	0.25
	1.56	1.25	2.15	1.45
		1.5	0.75	0.61
		1.75	0.47	0.40
CSCM	1.0	1.25	1.38	1.08
		1.5	0.66	0.49
		1.75	0.45	0.35
	1.56	1.25	3.7	2.61
		1.5	1.5	1.23
		1.75	0.77	0.57

It may be inferred that the geometry influences the displacements under blast loading. The apsidal unit can be considered more robust due to its inherent geometrical configuration. For a blast resistant configuration, an apsidal shape can thus be considered. This is in clear agreement with the fact that the apsidal units have relatively higher stiffness compared to the cylindrical units.

5.3. Constitutive model wise comparison

The simulation results for both the RHT and CSCM concrete constitutive models are compared here. The comparison for specific charge weights and standoff distances is given in Table 5.

Table 5. Peak displacement comparison – Concrete constitutive model wise

Structural Unit	Charge weight (kg)	Standoff distance R (m)	Peak displacement at DN1 (mm)	
			RHT model	CSCM model
Cylindrical	1.0	1.25	0.64	1.38
		1.5	0.38	0.66
		1.75	0.27	0.45
	1.56	1.25	2.15	3.70
		1.5	0.75	1.50
		1.75	0.47	0.77
Apsidal	1.0	1.25	0.52	1.08
		1.5	0.35	0.49
		1.75	0.25	0.35
	1.56	1.25	1.45	2.61
		1.5	0.61	1.23
		1.75	0.40	0.57

The values given in Table 4 clearly indicate that the CSCM concrete constitutive model returns conservative values of the displacement compared to the RHT model for the same charge weights and standoff distances for both cylindrical and apsidal units. For cylindrical unit, the displacement values are higher on average by 81.98% for the CSCM constitutive model. This difference in the apsidal unit is only 68.64% on average.

A graphical portrayal of these variations is representatively indicated in Fig. 5–8 for a charge weight of 1.56 kg and standoff distance of 1.25 m.

5.4. Parametric study

This study considers the displacement response of structural units to blast loading involving changes in the scaled distance, concrete constitutive model and the structural shape adopted for the simulations. The response is measured as the displacement at DN1, a node located on the top inner face of the structural units.

The displacement response for specific scaled distances and the corresponding charge weights and the standoff distances are compared in Table 6. The displacements show a decline with increasing scaled distances. This reduction is on expected lines as the explosive energy reaching the target structure diminishes with increasing scaled distances. A closer analysis reveals that for reduced scaled distances, displacement values are higher for higher charge weights. Thus, it can be deduced that there is a direct correlation between the charge weight and displacement response, and it is the charge weight that is the prime influencer.

Two distinct constitutive material models for concrete, namely the RHT and CSCM models were used in this research. The comparison of results is indicated in Table 5 and representatively in Fig. 7 and Fig. 8. The concrete constitutive models differ in the approach towards the loading rates encountered in blast loading. Higher loading rates result in an apparent increase

Table 6. Displacement comparison as per scaled distances

Scaled distance ($m/kg^{1/3}$)	**Charge weight (kg)**	**Standoff distances (m)**	**Peak displacement at DN1 (mm) – RHT**		**Peak displacement at DN1 (mm) – CSCM**	
			Cylindrical	Apsidal	Cylindrical	Apsidal
1.140	1.560	1.25	2.15	1.45	3.70	2.61
1.322	1.000	1.25	0.64	0.52	1.38	1.08
1.368	1.560	1.50	0.75	0.61	1.50	1.23
1.587	1.000	1.50	0.38	0.35	0.66	0.49
1.596	1.560	1.75	0.47	0.40	0.77	0.57
1.851	1.000	1.75	0.27	0.25	0.45	0.35

in strength. In the RHT model, this is accounted for by expanding the yield surface so that higher stress levels are required to reach the increased strength levels. The CSCM model adopts a viscoplastic approach that better matches stress transients prior to reaching the steady state strength [27]. The distinct behaviour of the two models contributes to the difference in the responses observed in the simulations. The RHT model requires higher stress levels for consideration of dynamic strengths and hence returns lower displacement values for the instances considered in this simulation.

The study utilises two distinct shapes – cylindrical and apsidal and the displacement responses are compared. This comparison is shown in Table 4 and in Fig. 5 and Fig. 6. As indicated in Section 5.2, the cylindrical unit undergoes higher displacement. Structural shape plays a key role in the interaction effects under blast loading. This is fundamental to the way in which the blast wave behaves when encountering an object in its path.

A blast wave on encountering a solid surface, will reflect from it and, depending on its geometry and size, diffract around it [28]. Further transit of the blast wave across the intervening structure creates rarefaction waves and vortices at the corners. The rarefaction wave attenuates the reflected wave and contributes to its decline [29]. For a cylindrical surface as is considered in this study, the incident wave and the reflected wave are joined by a Mach stem [29]. This effect weakens the reflected wave. Further passage of the blast wave generates a slipstream and vortices at the rear end.

This study features two distinctly curved shapes. In the apsidal shaped unit, the surface that is immediately exposed to the blast is curved in shape, but the side walls are orthogonal. This transition of the geometry may result in generating rarefaction waves lowering the effect of the reflected wave. This phenomenon is unlikely in a cylindrical unit. This exposes the cylindrical unit to relatively higher reflected pressure. However, this aspect needs to be subjected to further research and correlation.

It may be inferred that the geometry influences the displacements under blast loading. The apsidal unit can be considered more robust due to its inherent geometrical configuration. For a blast resistant configuration, an apsidal shape can thus be considered. This is in clear

agreement with the fact that the apsidal units have relatively higher stiffness compared to the cylindrical units.

A comparison of the displacement response across all the structural shapes, charge weights and standoff distances clearly indicates that an apsidal shaped concrete unit displays the least displacement response and thereby resists the blast loading better. The simulations also indicate that RHT constitutive models augments the findings in that the lower values of displacements

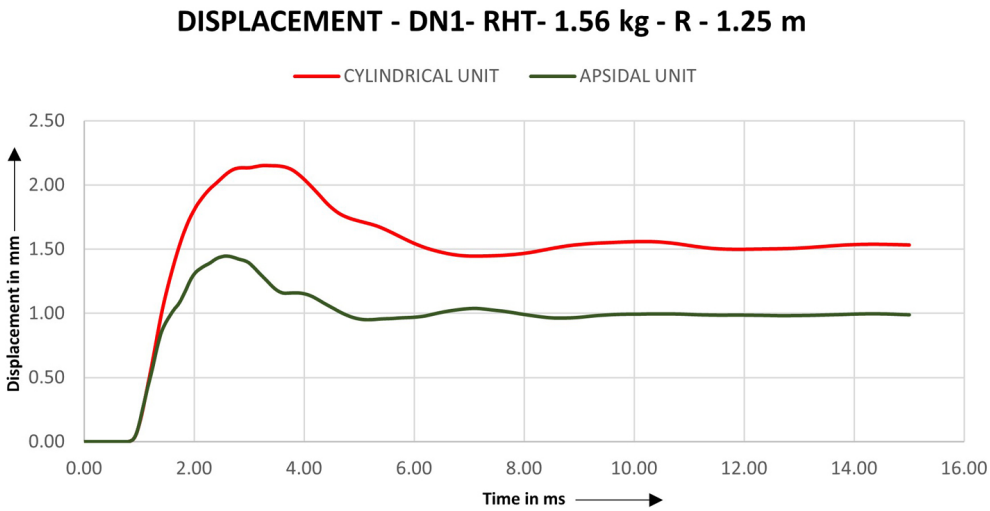

Fig. 5. Comparison of displacements at DN1 – RHT model

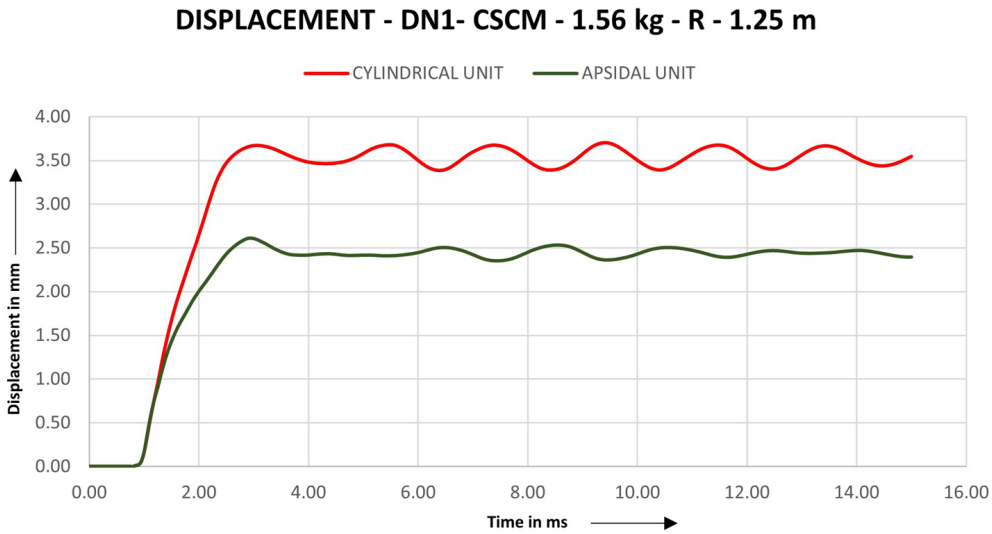

Fig. 6. Comparison of displacements at DN1 – CSCM model

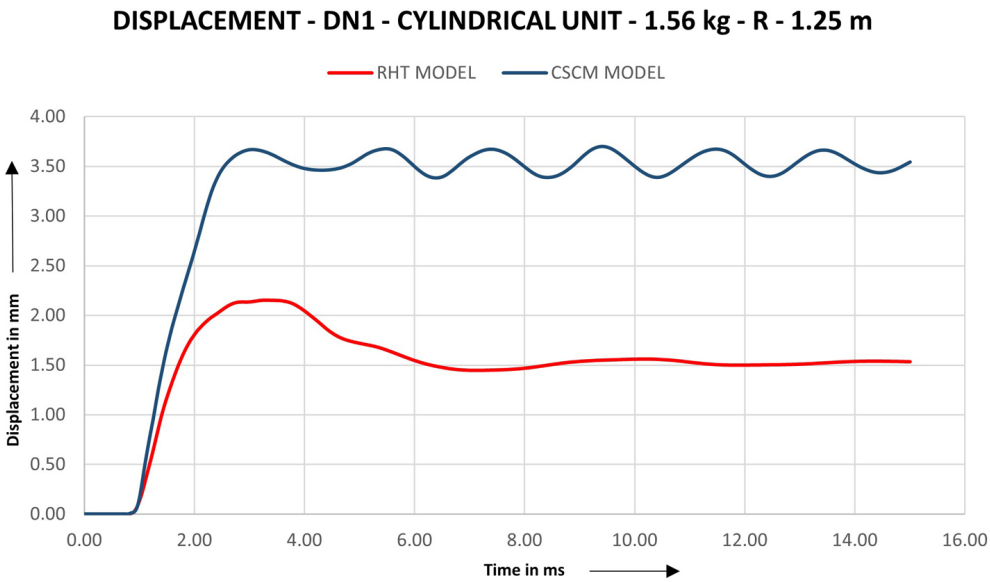

Fig. 7. Comparison of displacements at DN1 – Cylindrical unit

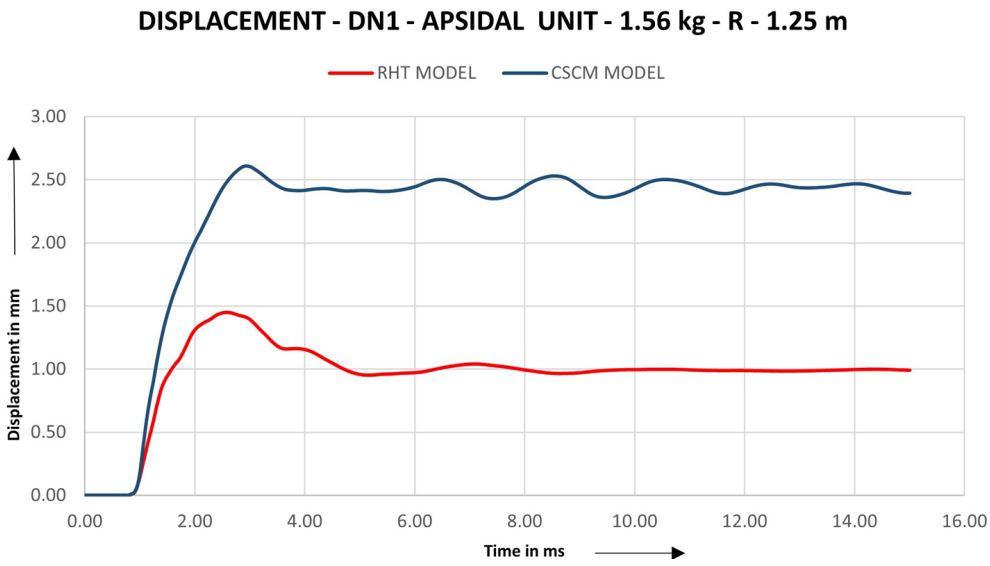

Fig. 8. Comparison of displacements at DN1 – Apsidal unit

are confirmed. Hence this study recommends an apsidal shaped concrete structural model and the use of RHT constitutive model in the consideration for a blast resistant environment.

6. Conclusions

The structural response of two distinct shaped concrete units under blast loading is evaluated using a parametric study incorporating two different concrete constitutive models. A total of twenty four simulations are carried out involving changes in the parameters - scaled distance, concrete constitutive model and the structural shape.

The structural shapes selected are both curved on the frontal face, but the apsidal unit, a unique shape, has orthogonal sides. The apsidal unit in its displacement response, performs better across all the simulations involving different charge weights and standoff distances. The complex interactions of the blast wave with the structure, attenuation of the reflected wave and the higher stiffness, results in this outcome. This provides a good indicator of the increased blast resistance of the apsidal unit.

The CSCM constitutive model returns conservative values of the displacement response as compared to the RHT model. Both models are well suited to analyse this scenario of blast loaded structural units. This study recommends the use of an apsidal structural unit modelled with a RHT constitutive model for concrete.

Further numerical studies involving structural units with varied dimensions and possible experimental work are required to substantiate and bolster the findings recorded here. This may be the subject of further work of this research.

References

[1] I.E. Edri, D.Z. Yankelevsky, A.M. Remennikov, and O. Rabinovitch, "Combined theoretical and experimental study on the blast response of arching masonry walls", *International Journal of Impact Engineering*, vol. 174, art. no. 104495, 2023, doi: 10.1016/j.ijimpeng.2023.104495.

[2] M. Kristoffersen, K.O. Hauge, A. Minoretti, and T. Borvik, "Experimental and numerical studies of tubular concrete structures subjected to blast loading", *Engineering Structures*, vol. 233, art. no. 111543, 2021, doi: 10.1016/j.engstruct.2020.111543.

[3] C. Fallon and G.J. McShane, "Fluid-structure interactions for the air blast loading of elastomer-coated concrete", *International Journal of Solids and Structures,* vol. 168, pp. 138–152, 2019, doi: 10.1016/j.ijsolstr.2019.03.017.

[4] P. Baranowski, M. Kucewicz, J. Malachowski, and P.W. Sielicki, "Failure behavior of a concrete slab perforated by a deformable bullet", *Engineering Structures*, vol. 245, art. no. 112832, 2021, doi: 10.1016/j.engstruct.2021.112832.

[5] Y.E. Ibrahim and M. Almustafa, "Mitigation of blast load risk on reinforced concrete structures considering different design alternatives", *Archives of Civil Engineering*, vol. 66 , no. 3 , pp. 225–238, 2020, doi: 10.24425/ace.2020.134394.

[6] S.A. Ismail, W. Raphael, E. Durand, F. Kaddah, and F. Geara, "Analysis of the structural response of Beirut port concrete silos under blast loading", *Archives of Civil Engineering*, vol. 67, no. 3 , pp. 619–638, 2021, doi: 10.24425/ace.2021.138074.

[7] M. Kucewicz, P. Baranowski, L. Mazurkiewicz, and J. Malachowski, "Comparison of selected blasting constitutive models for reproducing the dynamic fragmentation of rock", *International Journal of Impact Engineering,* vol. 173, art. no. 104484, 2023, doi: 10.1016/j.ijimpeng.2022.104484.

[8] C. Reifarth, R. Castedo, A.P. Santos, M. Chiquito, L.M. Lopez, A. Perez-Caldentey, S. Martinez-Almajano, and A. Alanon, "Numerical and experimental study of externally reinforced RC slabs using FRPs subjected to close-in blast loads", *International Journal of Impact Engineering,* vol. 156, art. no. 103939, 2021, doi: 10.1016/j.ijimpeng.2021.103939.

[9] M. Teich and N. Gebbeken, "Analysis of FSI effects of blast loaded flexible structures", *Engineering Structures*, vol. 55, pp. 73–79, 2013, doi: 10.1016/j.engstruct.2011.12.003.

[10] P. Baranowski, J. Malachowski, and L. Mazurkiewicz, "Local blast wave interaction with tire structure", *Defence Technology*, vol. 16, no. 3, pp. 520–529, 2020, doi: 10.1016/j.dt.2019.07.021.

[11] L. Mazurkiewicz, J. Malachowski, and P. Baranowski, "Optimization of protective panel for critical supporting elements", *Composite Structures*, vol. 134, pp. 493–505, 2015, doi: 10.1016/j.compstruct.2015.08.069.

[12] J. Li, C. Wu, and H. Hao, "An experimental and numerical study of reinforced ultra-high performance concrete slabs under blast loads", *Materials & Design*, vol. 82, pp. 64–76, 2015, doi: 10.1016/j.matdes.2015.05.045.

[13] M. Li, Z. Zong, H. Hao, X. Zhang, J. Lin, and G. Xie, "Experimental and numerical study on the behavior of CFDST columns subjected to close-in blast loading", *Engineering Structures*, vol. 185, pp. 203–220, 2019, doi: 10.1016/j.engstruct.2019.01.116.

[14] X. Lin, Y.X. Zhang, and P.J. Hazell, "Modelling the response of reinforced concrete panels under blast loading", *Materials & Design*, vol. 56, pp. 620–628, 2014, doi: 10.1016/j.matdes.2013.11.069.

[15] L. Mao, S.J. Barnett, A. Tyas, J. Warren, G.K. Schleyer, and S.S. Zaini, "Response of small scale ultra high performance fibre reinforced concrete slabs to blast loading", *Construction and Building Materials*, vol. 93, pp. 822–830, 2015, doi: 10.1016/j.conbuildmat.2015.05.085.

[16] G. Thiagarajan, A.V. Kadambi, S. Robert, and C.F. Johnson, "Experimental and finite element analysis of doubly reinforced concrete slabs subjected to blast loads", *International Journal of Impact Engineering*, vol. 75, pp. 162–173, 2015, doi: 10.1016/j.ijimpeng.2014.07.018.

[17] N. Gebbeken and T. Döge, "Explosion protection – Architectural design, urban planning and landscape planning", *International Journal of Protective Structures*, vol. 1, no. 1, pp. 1–21, 2010, doi: 10.1260/2041-4196.1.1.1.

[18] M. Barakat and J.G. Hetherington, "New architectural forms to reduce the effects of blast waves and fragments on structures", in *Proceedings of the International Conference on Structures under Shock and Impact*, *June 1998, Thessaloniki, Greece*. Southampton: WIT Press, 1998, pp. 53–62.

[19] N. Rouzsky, "Blast-resistant control buildings", *Structural Safety*, vol. 5, no. 4, pp. 253–266, 1988, doi: 10.1016/0167-4730(88)90027-6.

[20] T. Borrvall and W. Riedel, "The RHT concrete model in LS-DYNA", in *Proceedings of the* 8^{th} *European LS-DYNA Users Conference, May 2011, Strasbourg*. [Online]. Available: https://www.dynalook.com/conferences/8th-european-ls-dyna-conference/session-12/Session12_Paper1.pdf. [Accessed: 18 Aug. 2023].

[21] Y.D. Murray, *Users manual for LS-DYNA concrete material model 159, Publication no. FHWA-HRT-05-062*. McLean, VA, USA: US Department of Transportation, Federal Highway Administration, 2007.

[22] LS DYNA – Keyword User's Manual R13: Livermore Software Technology, Livermore, California, USA, 2021.

[23] Superpower 90 – Solar group packaged explosives: Solar Industries India Limited, Nagpur, India.

[24] J. Henrych, The dynamics of explosion and its use. Amsterdam, Netherlands: Elsevier Scientific Publishing Company, 1979.

[25] ASCE, Design of blast-resistant buildings in petrochemical facilities. Reston, VA, USA: American Society of Civil Engineers, 2010.

[26] UFC 3-340-02, Structures to resist the effects of accidental explosions. Washington DC , USA: US Department of Defense, 2008.

[27] R.M. Brannon and S. Leelavanichkul, *Survey of Four Damage Models of Concrete*. Albuquerque, NM, USA: Sandia National Laboratories, 2009.

[28] D. Cormie, G. Mays, and P. Smith, *Blast effects on buildings*. London, UK: ICE Publishing, 2012.

[29] W.E. Baker, *Explosions in air*. Austin, TX, USA: University of Texas Press, 1973.

Received: 2025-01-16, Revised:2025-01-28